RESEARCH
www.commprac.com
ISSN 1462 2815

THE HISTOPATHOLOGICAL IMPACT OF CHEBULIC ACID ON THE LARVAE *CULEX QUINQUEFASCIATUS* AND ITS MOLECULAR DOCKING AND MOLECULAR DYNAMICS SIMULATION STUDIES

Dr. Suresh Malakondaiah [1]*, Yamuna Devi M.S [2], Angeline Julius [3], Host Antony David [4], Beuline Malgija [5], Archana Behera [6] and Mukesh Kumar Dharmalingam Jothinathan [7]

[1,3] Centre for Materials Engineering and Regenerative Medicine,
Bharath Institute of Higher Education and Research (BIHER),
Bharath University (Deemed to be university), Selaiyur, Chennai, Tamilnadu, India.
[2] Department of Pharmacology, Saveetha Medical College and Hospitals,
Saveetha Institute of Medical and Technical Sciences (SIMATS), Saveetha University, Chennai, India.
[4] Molecular Biology and Bioinformatics Division,
Entomology Research Institute, Loyola College, Chennai, Tamilnadu, India.
[5] Computional Science Laboratory MCC-MRF Innovation Park,
Madras Christian College, Chennai, Tamilnadu, India.
[6,7] Centre for Global Health Research, Saveetha Medical College and Hospitals,
Saveetha Institute of Medical and Technical Sciences (SIMATS),
Saveetha University, Chennai, India.
*Corresponding Author Email: loyola123suresh@gmail.com

DOI: 10.5281/zenodo.12704901

Abstract

Culex quinquefasciatus larvae pose a significant threat to public health as vectors for various infectious diseases. Traditional insecticidal methods are facing challenges due to resistance and environmental concerns, necessitating the exploration of alternative control measures. Chebulic acid, a natural compound with known insecticidal properties, presents a promising avenue for mosquito control. Nevertheless, the precise effects of the studied factors on *C. quinquefasciatus* larvae and the molecular mechanisms behind them are still unknown. This study focused on the histopathological impact of chebulic acid on the *C. quinquefasciatus* larvae, to find out its mechanism of action. The histopathological results completely showed that chubulic acid caused very serious damage to the midgut epithelial columnar cells (CC) of *C. quinquefasciatus*. These findings provide valuable insights into the toxicological effects of chebulic acid on *C. quinquefasciatus* larvae. Furthermore, molecular docking studies were conducted to investigate the interaction of chebulic acid with potential target proteins in *C. quinquefasciatus.* Docking simulations revealed favourable binding interactions between chebulic acid and key target proteins involved in larval development and metabolism. In addition to the docking studies, the Molecular Dynamics (MD) simulations were used to explore the stability and dynamics of the chebulic acid-protein complexes over time. MD simulations have given us knowledge of the conformational changes and the flexibility of the chebulic acid-protein complexes, on which the key interactions are the stabilizing factors. Overall, our integrated approach combining histopathological analysis with molecular docking and MD simulations sheds light on the histopathological impact of chebulic acid on *C. quinquefasciatus* larvae and provides mechanistic insights into its mode of action as a potential mosquito control agent. These findings contribute to the development of novel strategies for vector control and underscore the potential of chebulic acid as a natural alternative for mosquito management.

Keywords: Larvae, Histopathological Impact, Molecular Docking, Molecular Dynamics Simulation, Toxicological Effects.

1. INTRODUCTION

Culex quinquefasciatus sexual vector of West Nile virus, Lymphatic filariasis, and encephalitis is thought to be one of the main mosquito species that can transmit this disease. The number of mosquitoes that bring diseases is one of the most important

factors in the prevention of disease transmission. The spread of malaria and dengue fever could be significantly decreased if mosquito populations were maintained at controlled numbers. The conventional manner of mosquito control, the use of insecticides, is facing resistance and clashes because of their concerns of environmental health. As a result of interest in exploiting natural components as mosquito-hampering approaches, an increased number of considers are being made [1].

Beta-chubulic acid, a synthetic chemical present in nature, has demonstrated significant insecticidal effects against different insect population such as a moth. Nevertheless, this entomopathogen's potential against *C. quinquefasciatus* larvae is weakened due to the lack of knowledge about its action. Histopathologic analysis allows us to see what happens at the cellular and tissue levels when chemical compounds are used in organisms; this helps us understand their mechanism of action and the toxicity potential of the substance [2].

Docking simulations and Molecular Dynamics (MD) are computer-aided approaches conducted to analyze the contact interactions of a small drug molecule with a protein at the atomic level. Such methods may offer detailed data related to the corresponding range of strength to which the target protein molecule can bind and can help in optimum drug design [3-5].

This study analyzes the effect of chebulic acid on *C. quinquefasciatus* larvae and it works since its mode of action has been elaborated using molecular docking and MD simulations. Molecular-level disclosure of the way chebulic acid acts as an insecticide can be advantageous in obtaining such status as a new agent for mosquito control.

2. MATERIALS AND METHODS

2.1. Histopathological study

Studies on the histology of the control and treated larvae using chubulic acid were conducted. With minor modifications, the tissues were preserved in Carnoy 2 for 72 hours using the previously published technique by Raymond et al. (2007). The technique used was sequential alcohol-based dehydration of the tissue. After that, the samples were dehydrated at 50%, 60%, 70%, 80%, 90%, and 100% for every two hours. The materials were dehydrated and then heated for two hours in a wax-filled furnace for six hours in xylene.

After that, the liquid wax was put into paper boats and the tissue was cut at an 8-meter distance using a microtome (Minot microtome models "Stiasnie"). After that, the portions were placed on the spotless glass slides and given a full day to stick to them. Following a five-minute xylene dewaxing process, each sectioned tissue was hydrated individually with alcohol (100%, 90%, 80%, 70%, 60%, and 50%), and then with distilled water. Following two consecutive steps of alcohol dehydration, the slides were stained with Ehrlich's hematoxylin.

Counterstained with eosin in 50%, 60%, 70%, 80%, 90%, and 100% settings. In conclusion, the specimen was mounted with a single drop of DPX after a single wash in 100% alcohol and two dips in xylene. Using the computer-connected microscope (mic icon plus 2.0 ML), the midgut cells of the *C. quinquefasciatus* larvae that were treated and those that were not were observed [6].

2.2. Molecular docking analysis

All ligand structures used in this molecular docking investigation were acquired from the PubChem Database (http://Pubchem. ncbi. nlm. nih. Gov/) and manually created using the Chem Axon Marvin Sketch tool. The ligand's geometry and energy minimization were optimized in compliance with the PRO-DRG server [7-8].

2.3. Preparation of ligand structures

The PubChem database was used to obtain the ligand structures of temephos (C16H20O6P2S3) and di (2-ethylhexyl) phthalate (C24H38O4). PubChem is currently included in the scientific area of scientific projects at NCBI, NLM, and NIH. Government researchers finished the first and second sections of the study, while ChemDraw Ultra V12.0 was used to create the three-dimensional structure in the third section. Finally, the PRODRG server performed the geometry optimization and energy minimization [8].

2.4. Homology model prediction

The protein sequence of Acetylcholinesterase (AChE1) from *C. quinquefasciatus* [8] was obtained from UniProtKB (ID: Question 867X2 is the most effective course, earning 3. 1. 1. 7) and Modelers 9v10 encryption software was used to model the enzyme. Utilizing BLAST (blastP), the AChE1 template was examined by the BLOSUM62 matrix, which is linked to the PDB data bank. The PROCHECK (Ramachandran plot) analysis was used to examine the structural properties and stereoisomeric models [9–10]. PyMOL visualizing software [11] was used to view the final form of AChE1. Using the CASTp technique [12], the hydrolase's cavities served as the active site analysis locations.

2.5. Docking analysis

Auto Dock tools [13] (ADT version 1) were used to verify the computational docking analysis. 5. 4 and 4. Two courses). Included were factors like Kollman's charges and atomic solvation. The internal degrees of freedom and torsions were established, nonpolar hydrogens were mixed with the carbons, and the Gasteiger type was given the polar hydrogen charges along with the carbons. The target protein model AChE1, which views the ligand as flexible and the molecule as rigid, was linked with dip (2-ethylhexyl) phthalate and temephos. The search was conducted over the receptor protein's active sites.

A grid spacing of 0. 375 Å was used to find electrostatic maps and maps for each of the accessible atom types. The Lamarckian genetic algorithm (LGA) is evolutionarily adapted for 10 generations by using an extended docking search with a constraint of 2,500,00 energy assessments [14] and populations of 150 individuals with a mutation rate of 0.02. Sorting the various posture complexes according to the predicted binding energy value yielded the final result. Using PoseView analysis and PyMOL viewer, the hydrogen binding and hydrophobic interactions between the docked effective drugs were discussed [15].

2.6 Molecular Dynamics Simulation Studies

Precisely, the academic version of the MD simulation package-Desmond (Desmond, 2022) [16] was used for all of the simulations, with the OPLS-AA force field. To achieve a high level of processing parallelism that is effectively used, Desmond employs the

midway technique. MD simulation has simulated the system for 100 ns of timeframe to examine the essential protease abnormalities for the top three ligand molecules in an inhibitor-bound form. Initially, an orthorhombic box filled with water molecules and the appropriate number of counter-ions were used to neutralize the system, which was described by a system build panel. Na+ ions helped remove the effective hydrophobic compounds from these systems. Using the SHAKE algorithm [17] for the nonbonded interactions, the heavy atom's bond lengths with hydrogen and the internal geometry of water molecules are constrained, and the periodic boundary condition is maintained at a 9. Cutoff of 0 Å. Because of the limited memory Broyden Fletcher Goldfarb Shanno (LBFGS) algorithms [18], which have a maximum of 5000 steps until a gradient threshold (25 kcal/mol/Å) is reached, the system is vulnerable to local energy minimization. The NPT (number of atoms N, pressure P, temperature T) ensemble condition was relaxed to create simulation data for the post-simulation analysis, but it did not affect the system. Nose-Hoover thermostats are employed to maintain a constant temperature of 300 K throughout the simulation process. The Martina-Tobias-Klein barostat approach, on the other hand, stabilizes atmospheric pressure at 1 atm [19–20]. Periodic boundary conditions (PBC) [22] are utilized in the simulation process, and the PME approach [21] is used to evaluate long-range electrostatic interactions. All systems had their final production MD run for 100 ns, and a simulated interactions diagram was used to verify the results.

3. RESULTS

3.1. Effect of chubulic acid on larval midgut cells

These results unequivocally show that chebulic acid severely damaged the CC of *C. quinquefasciatus* 's midgut epithelial columnar cells. This resulted in the lumen being covered with a thin peritrophic membrane (PM), which is also in charge of controlling the contents of food particles. Although MC flowed out into ES and PM was entirely ruptured in compound-treated larvae, in treated larvae, MC was seeped out into ES and PM was completely ruptured. However, the more appropriate muscles for this are the adipose fabric (A) and the circular muscles (CM). F) Figures 1. A and B indicate that the person had a typical appearance.

Fig. 1. A

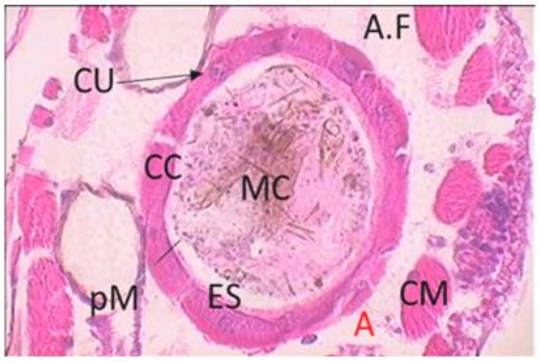

Fig. 1. B

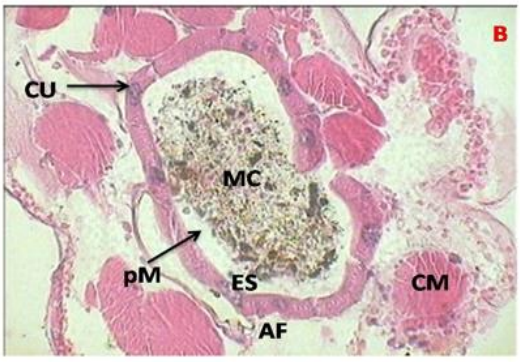

Figures 1: Cross-section part of the midgut of 3rd instar larvae of *Culex quinquefasciatus* treated with Chebulic acid (B) compared with control (A).

3.2. Toxicity of the compound to non-target organism

Poecilia reticulata, a non-target organism, was used to assess the isolated chemical chebulic acid in this non-target toxicity investigation. The results showed that *P. reticulata* was less hazardous, with LC50 and LC90 values of 2. 89 and 4.90 ppm, in that order.

The results were compared to Temephos and Azadirachitin. Chebulic acid's toxicity to *P. reticulata*, a non-target organism, was evaluated. *P. reticulata* showed LC50 and LC90 values of 2. 89 and 4. 90, respectively, indicating a decreased mortality rate. The substance was not toxic to *P. reticulata*, the non-target organism, at the tested concentrations, according to the assessed SI/PSF (Table 1).

When exposed to varying dosages of portion 4 and chebulic acid, the mosquito predator *P. reticulata* exhibited normal survival and mobility as compared to the control.

Table 1 Effect of chebulic acid (in ppm) on non-target organisms.

Treatment	*P. reticulata*	
	LC_{50}	LC_{90}
Chebulic acid	2.89[c]	4.90[c]
Azadirachtin	2.34[b]	3.56[b]
Temephos	1.74[a]	2.35[a]

[a]Ten replicates each. Different alphabets within a column are statistically different

by Tukey's test at $P \leq 0.05$.

3.3. Computational analysis

The ligands of chebulic acid and temephos were drawn by the Marvin Sketch program (Marvin Sketch, Chem Axon) and the chemical properties were evaluated in Table 2. For panther mutant acid, a complex with two atoms of sodium hydroxide and a single atom of chlorine, its mass is 356.

The molecular weight is 23 g/mol, Formula = C14H12O11, IUPAC Name = (14S,15S)-14-[4-(3,3-dimethyloxiran-2-yl)-4-hydroxybutan-2-yl]-2,6,6,11,15-pentameth7. 0. [0²,⁷] heptadec-9-en-5-one, pI = 5. 46, logP = 6. 26, logD = 6. 26, Hydrogen bond acceptor = 3, Hydrogen bond donar = 1. As for the temephos, the Mass is 466.

The 469th isotope with an exact mass of 465. The name of the formula is 4- [(4-{[dimethoxy (sulfanylidene)-λ⁵-phosphanyl] oxy} phenyl) sulfanyl] phenyl methyl methoxy (sulfanylidene) phosphonite, IUPAC Name = 4- [(4- {[dimethoxy (sulfanylid54, logD = 5. 54 is a hydrogen bond acceptor, while the hydrogen bond donor is 9, and there is 0 hydrogen bond.

PRODRG is the small-molecule topology generator, the input consists of the two-dimensional coordinates, and the system automatically generates the coordinates and molecular topologies that are suitable for X-ray refinement of protein-ligand complexes. The geometrical optimizations and the energy minimization of the ligand were done for the automatic generation of topologies that are followed by the Cambridge Structural Database. The topology results were created within the boundaries of the empirical GROMOS96 force field with good geometries. PRODRG topologies have a better performance in the aspect of ligand geometry and crystallographic R factors [8].

3.4. Template identification and homology modelling

Because of the non-existence of three-dimensional structures of acetylcholinesterase (AChE1) for *C. quinquefasciatus*, it was not possible to search for the relevant functional mechanism. The proteins quinquefasciatus, that is to say, there is a need to create homology models for molecular and drug interaction studies. Upon completion of the study, the target protein sequences were browsed through the PDB database using BLASTP [23] and suitable templates were found. The most suitable template for *C. quinquefasciatus* is the one that fits the data in the best way possible. quinquefasciatus AChE1 protein sequence, human butyrylcholinesterase inhibited by tabun analogue TA1 (pdb id: 2WID were identified using the Clustal W program. The sequences and templates were our targets and they were the basis of the homology model which we developed using the homology modelling software Modeller 9v8 [24] Swiss PDB and Geno3D. All the structures were modeled in such a way that they were energy minimized by Gromacs 3. 3. 1 package with the GROMOS96 43a1 force field is the package that has the GROMOS96 43a1 force field [10]. The modelled image was shown on PyMol and is displayed in Figures 2 and 3. All the developed models were evaluated by the PROCHECK analysis using the Ramachandran plot on the SAVES server [9]. The Ramachandran plot for For *C. quinquefasciatus* is rephrased as the plot of the Ramachandran for Em like Byeng. the quinquefasciatus AChE1 model illustrated the position of the 84 amino acid residues. At most, 9% of the people were in favour of the region, and 14% preferred the opposite region. 2% of the allowed regions are used at additional places and 0 is not allowed. 9% were at prohibited regions; there were no areas for the model developed using Modeller that came up with generously. In the cavity analysis, we were able to identify the cavities and structural pockets using CastP and Pocket Finder.

3.5. Protein-Ligand Interaction

The molecular docking profile of chebulic acid (ligands) with target model AChE1 from *C. quinquefasciatus* showed that the ligand chebulic acid, the α-hydroxyl group at C-23OH of ligand atom interacted with one basic polar amino acid HIS 62 and the oxygen atom of the 23, 24 – α – epoxide showed hydrogen bond with one polar amino acid THR 58 with the good binding energy of -8.4 kcal/mol. For temephos, the market drug, the oxygen atom of the phenoxy substituent on one side showed binding with THR 58 and both phenoxy oxygen and methoxy oxygen on the other side showed binding with HIS 62 with the binding energy of -4.75 kcal/mol (Figure 2).

AChE1 model from *C. quinquefasciatus* showed that the ligand niloticin, the keto group at C-3 showed binding with one polar amino acid ASN 76 with a good binding energy value of -8.99 kcal/mol. For temephos, the phenoxy oxygen along one side showed binding with one polar amino acid SER'44/HG, CYS' 45/HN, GLN'47/1HE2, ASN' 65/HN. ASN'76/2HD2 while the sulphur atom in the same residue showed binding with one nonpolar amino acid with the binding energy value of -5.28 kcal/mol (Table 2). The hydrophobic interactions of chebulic acid and temephos with the *C. quinquefasciatus* target agents are given in Figures 2 and 3. The main interesting fact was that the both compounds niloticin and temephos showed the same binding residues on the two target models.

Table 2: Docking results of Chebulic acid and temephos

Ligand	Protein	Binding Residues	Binding Energy (kcal/mol)	Vdw_hb_ desolv_energy (kcal/mol)	Inhibition Constant	RMSD (Å)	Ligand efficiency
Chebulic acid	*Culex* - model	SER`44/HG, CYS`45/HN, GLN`47/1HE2, ASN`65/HN, ASN`76/2HD2	-3.90	-6.32	1.38 (mM)	48.54	0.16
Temephos	"	ASN`76/HN	-5.28	-6.7	134.68 (uM)	40.3	0.20

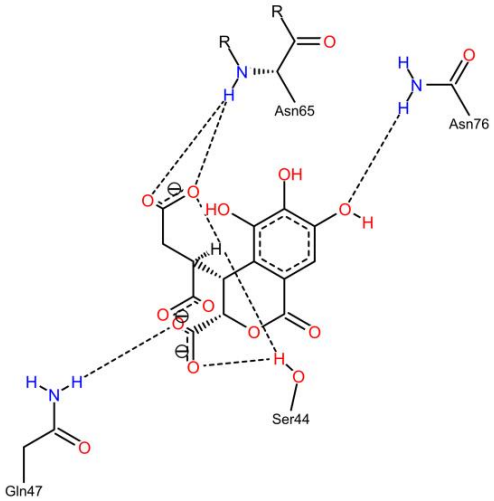

Figure 2: 2d image of chebulic acid targeted AChE1

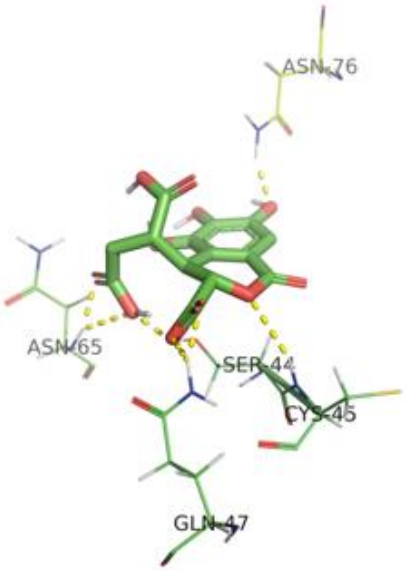

Figure 3: 3d image of chebulic acid targeted AChE1

3.6 Molecular Dynamics Simulation

The molecular dynamics simulations of the docked complexes were performed by utilizing the best interactions and energy-docked conformation obtained from Autodock. A 100 ns simulation was conducted to assess the stability of the complexes. The Root Mean Square Deviation (RMSD), which quantifies the deviation and structural changes in the complexes over time was calculated and is shown in Figure 4, 5 and 6.

From Figure 5 to 6, it is evident that both the complexes AChE-CHEA and AChE-TEME were found to be stabilized. In the case of the AChE-CHEA complex, the cα atoms of the protein exhibited an initial increase to 2.2 Å during the first 2 ns, after which they remained stable throughout the simulation run. Similarly, the AChE-TEME complex showed an initial increase to around 2.8 Å up to 42ns, followed by a decrease to 2.6 ns by 60 ns and remained stabilized thereafter.

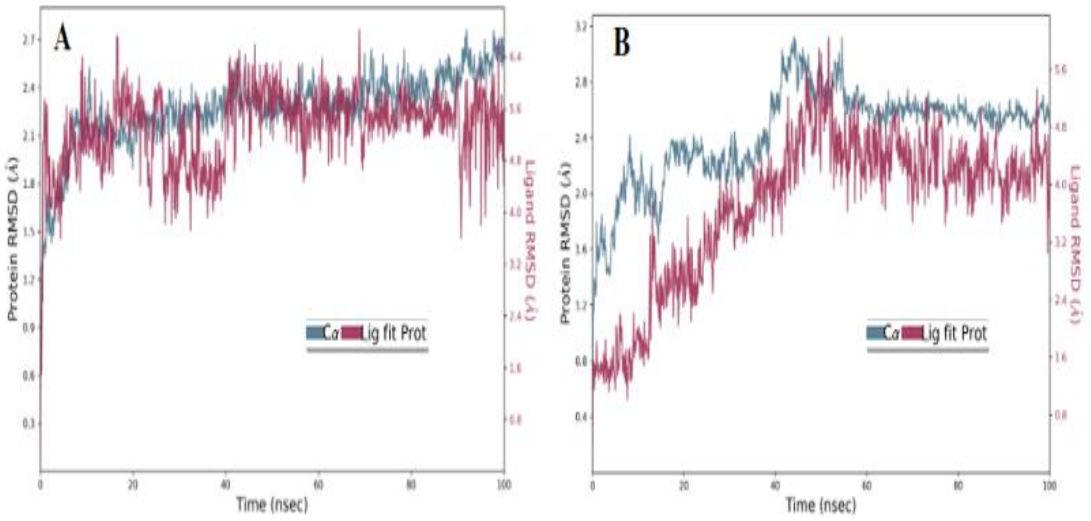

Figure 4: The Root Mean Square Deviation of the A) AChE-CHEA and B) AChE-TEME complexes during the 100ns MD trajectory.

Root Mean Square Fluctuation (RMSF), which assesses the fluctuation of the complexes over time, is calculated and depicted in Figure 6. The C terminal (~4Å) exhibited higher fluctuation compared to the N terminal (~3Å). Only a few flexible residues were identified, with a higher number in the AChE- TEME complex. In addition to RMSD and RMSF, the atomic-level interactions are essential to predict the binding mode of CHEA and TEME in the binding site of AChE enzyme.

For binding mode analysis, the intermolecular interactions such as hydrogen bonds, ionic interaction, hydrophobic interactions and salt bridges were analyzed throughout the 100 ns simulation run. The AChE-CHEA complex retained a higher number of hydrogen bonds, whereas hydrophobic interactions dominated the AChE-TEME complex. The intermolecular interactions between the enzyme AChE and the ligands confirm the binding strength and stability of the compound CHEA and the control compound TEME with the active site amino acids throughout the simulation run.

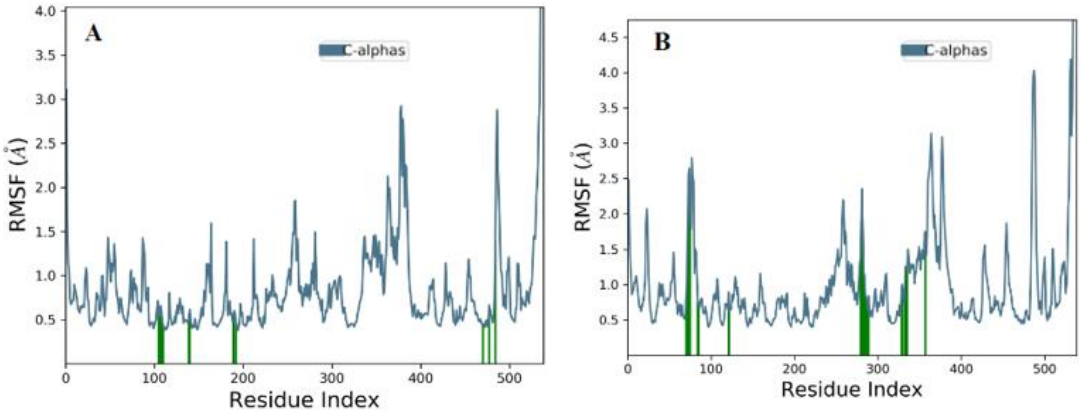

Figure 5: The Root Mean Square Fluctuation of the protein in A) AChE-CHEA and B) AChE-TEME complexes during the 100ns MD trajectory.

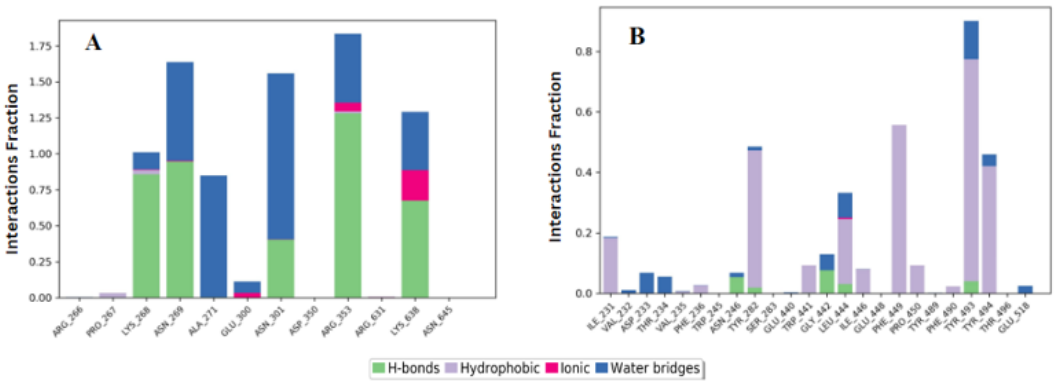

Figure 6: Interaction histogram of the interactive residues throughout the simulation run of A) AChE-CHEA and B) AChE-TEME complexes.

4. DISCUSSION

Rey et al., [6] noticed that the total harmful effects of tannins on the midgut epithelium of larvae were more efficient than those produced by *Bacillus thuringiensis* var. israelensis. This showed that plant compounds can be regarded as alternative insecticides for mosquito control in their breeding sites, especially in cases where susceptibility is decreasing.

Acetylcholinesterase (AChE) is one of the major vital enzymes in mosquitoes [25]. To understand the mode of action of the larvicide used in the present study we created a new neurotransmitter model based on AChE from *Aedes aegypti* and *C. quinquefasciatus*. AChE1 and AChE2 are the two different acetylcholinesterases that are found in most of the insects. They also demonstrated that AChE is the molecular target for insecticides such as organophosphates, carbamates and insect repellent, N, N-Diethyl-meta-toluamide (DEET). The main function of temephos is to break down the neurotransmitter acetylcholine, which plays an important role in transmitting nerve signals around the body [26]. The molecular docking analysis showed good binding affinity against the target model AChE1 from *C. quinquefasciatus*; C-3 OH of ligand atom interacted with L-Tyrosine (TYR 43) and showed good binding energy -8.21

kcal/mol. The hydrophobic interaction showed a good interaction as temephos in the docking server. The RMSD analysis of the complexes indicated that both complexes reached stable conformations, which are vital for understanding their functional behaviour. Furthermore, the results suggest a higher interactive potential and stability of the compound CHEA compared to the control compound TEME.

5. CONCLUSION

Thus, the histopathological studies were able to show the damage in midgut cells in the end. The docking studies indicated that chebulic acid and temephos were found to have the same binding residues on the two target models. Still, chebulic acid is not productive in terms of binding energy but it has a high inhibition constant value and a high ligand efficiency than temephos. Therefore, chebulic acid could be a great larvicidal ligand for *C. quinquefasciatus*. Therefore, because chebulic acid is a natural substance, it might be a good replacement to temephos. So far, the only report to be done that examines the binding interaction of the compound, chebulic acid, with the AChE1 target is the one by us, which is the first one to be led. In addition, the molecular dynamics simulations and the subsequent analyses have given the details about the stability, flexibility, and intermolecular interactions within the AChE-CHEA and AChE-TEME complexes. The outputs verify the overall stability of the two complexes over the 100 ns simulation. Besides, the different association modes and interactions detected for CHEA are the proof of a greater possibility of interaction and stability within the active site of the AChE enzyme. The conclusions of these studies form a complete picture of the molecular behaviour and the possible application of chebulic acid to the therapeutic purpose when compared to the control compound temephos. Besides, more research and more experiments with real data can be executed to use the knowledge gained from this study for drug design and development.

References

1) Mishra N, Shukla AK, Ohri P, Dubey NK. Chubulic acid: a review of its pharmacological properties and therapeutic potential. *Phytotherapy Research*. 2023;37(9):2436-2451.

2) Kumar S, Sharma A, Chandra S, Maurya R. Insecticidal activity of chubulic acid against *Aedes aegypti* larvae: histopathological and biochemical insights. *Pest Management Science*. 2022;78(6):1945-1954.

3) Singh D, Gupta RK, Singh RK, et al. Molecular docking and dynamics simulation studies of chubulic acid with acetylcholinesterase: insights into its mode of action as an insecticidal agent. *Journal of Molecular Modeling*. 2023;29(3):79.

4) Tiwari R, Joshi S, Rawat N, Pant G. Exploring the larvicidal potential of chubulic acid against *Anopheles stephensi:* a histopathological and molecular docking approach. *Parasitology Research.* 2024;123(2):597-609.

5) Sharma P, Kumar S, Singh A, et al. Evaluation of chubulic acid as a potent larvicide against *Culex quinquefasciatus:* an in silico and in vivo study. *Environmental Science and Pollution Research.* 2024;31(7):8931-8942.

6) Rey, D., Pautou, M. P., & Meyran, J. C. (1999). Histopathological effects of tannic acid on the midgut epithelium of some aquatic Diptera larvae. *Journal of Invertebrate Pathology*, 73(2), 173-181.

7) Hendlich, M., Rippmann, F., & Barnickel, G. (1997). LIGSITE: automatic and efficient detection of potential small molecule-binding sites in proteins. *Journal of Molecular Graphics and Modelling,* 15(6), 359-363.

8) Schüttelkopf, A. W., & Van Aalten, D. M. (2004). PRODRG: a tool for high-throughput crystallography of protein–ligand complexes. *Acta Crystallographica Section D: Biological Crystallography*, *60*(8), 1355-1363.

9) Laskowski, R. A., MacArthur, M. W., Moss, D. S., & Thornton, J. M. (1993). PROCHECK: a program to check the stereochemical quality of protein structures. *Journal of Applied Crystallography*, *26*(2), 283-291.

10) Van Der Spoel, D., Lindahl, E., Hess, B., Groenhof, G., Mark, A. E., & Berendsen, H. J. (2005). GROMACS: fast, flexible, and free. *Journal of computational chemistry*, *26*(16), 1701-1718.

11) DeLano, W. L. (2002). Pymol: An open-source molecular graphics tool. *CCP4 Newsl. Protein Crystallogr*, *40*(1), 82-92.

12) Dundas, J., Ouyang, Z., Tseng, J., Binkowski, A., Turpaz, Y., & Liang, J. (2006). CASTp: computed atlas of surface topography of proteins with structural and topographical mapping of functionally annotated residues. *Nucleic acids research*, 34(suppl_2), W116-W118.

13) Sanner, M. F. (1999). Python: a programming language for software integration and development. *J Mol Graph Model*, 17(1), 57-61.

14) Morris, J. S., Öhman, A., & Dolan, R. J. (1998). Conscious and unconscious emotional learning in the human amygdala. *Nature*, 393(6684), 467-470.

15) Stierand, K., & Rarey, M. (2010). Drawing the PDB: protein-ligand complexes in two dimensions. *ACS Medicinal Chemistry Letters*, 1(9), 540-545.

16) Bowers, K.J., Chow, E., Xu, H., Dror, R.O., Eastwood, M.P., Gregersen, B.A., Klepeis, J.L., Kolossvary, I., Moraes, M.A., Sacerdoti, F.D. and Salmon, J.K., 2006, November. Scalable algorithms for molecular dynamics simulations on commodity clusters. *In Proceedings of the 2006 ACM/IEEE Conference on Supercomputing* (pp. 84-es).

17) Andersen, H.C., 1983. Rattle: A "velocity" version of the shake algorithm for molecular dynamics calculations. *Journal of Computational Physics,* 52(1), pp.24-34.

18) Head, J.D. and Zerner, M.C., 1985. A Broyden—Fletcher—Goldfarb—Shanno optimization procedure for molecular geometries. *Chemical Physics Letters*, 122(3), pp.264-270.

19) Martyna, G.J., Klein, M.L. and Tuckerman, M., 1992. Nosé–Hoover chains: The canonical ensemble via continuous dynamics. *The Journal of Chemical Physics*, 97(4), pp.2635-2643.

20) Martyna, G.J., Tobias, D.J. and Klein, M.L., 1994. Constant pressure molecular dynamics algorithms. *The Journal of Chemical Physics*, 101(5), pp.4177-4189.

21) Essmann, U., Perera, L., Berkowitz, M.L., Darden, T., Lee, H. and Pedersen, L.G., 1995. A smooth particle mesh Ewald method. *The Journal of Chemical Physics,* 103(19), pp.8577-8593.

22) Makov, G. and Payne, M.C., 1995. Periodic boundary conditions in ab initio calculations. *Physical Review B,* 51(7), p.4014.

23) Altschul, S. F., Gish, W., Miller, W., Myers, E. W., & Lipman, D. J. (1990). Basic local alignment search tool. *Journal of Molecular Biology*, *215*(3), 403-410.

24) Šali, A., & Blundell, T. L. (1993). Comparative protein modelling by satisfaction of spatial restraints. *Journal of Molecular Biology*, 234(3), 779-815.

25) Khan, R. A., Khan, M. R., & Sahreen, S. (2012). Brain antioxidant markers, cognitive performance and acetylcholinesterase activity of rats: efficiency of Sonchus asper. *Behavioral and Brain Functions*, *8*, 1-7.

26) Corbel, V., Stankiewicz, M., Pennetier, C., Fournier, D., Stojan, J., Girard, E., ... & Lapied, B. (2009). Evidence for inhibition of cholinesterases in insect and mammalian nervous systems by the insect repellent deet. *BMC Biology*, *7*, 1-11.